Acid/Base Switching of the Tautomerism and Conformation of a Dioxoporphyrin for Integrated Binary Subtraction

ARTICLE *in* CHEMISTRY - A EUROPEAN JOURNAL · SEPTEMBER 2014

Impact Factor: 5.73 · DOI: 10.1002/chem.201403830

9 AUTHORS, INCLUDING:

Yubin Ding
Nanjing University
17 PUBLICATIONS **506** CITATIONS
SEE PROFILE

Jonathan P Hill
National Institute for Materials Science
286 PUBLICATIONS **8,686** CITATIONS
SEE PROFILE

Katsuhiko Ariga
National Institute for Materials Science
623 PUBLICATIONS **21,611** CITATIONS
SEE PROFILE

Hans Agren
KTH Royal Institute of Technology
867 PUBLICATIONS **18,728** CITATIONS
SEE PROFILE

ChemPubSoc Europe

DOI: 10.1002/chem.201403830

CHEMISTRY A European Journal Full Paper

Logic Devices

Acid/Base Switching of the Tautomerism and Conformation of a Dioxoporphyrin for Integrated Binary Subtraction

Yubin Ding,[a] Xin Li,[b] Jonathan P. Hill,[c] Katsuhiko Ariga,[c] Hans Ågren,[b] Joakim Andréasson,[d] Weihong Zhu,[a] He Tian,[a] and Yongshu Xie*[a]

Abstract: Compared with most of the reported logic devices based on the supramolecular approach, systems based on individual molecules can avoid challenging construction requirements. Herein, a novel dioxoporphyrin **DPH_{22}** was synthesized and two of its tautomers were characterized by single-crystal X-ray diffraction studies. Compound **DPH_{22}** exhibits multichannel controllable stepwise tautomerization, protonation, and deprotonation processes through interactions with H^+ and F^- ions. By using the addition of H^+ and F^- ions as inputs and UV/Vis absorption values at $\lambda = 412$, 510, 562, and 603 nm as outputs, the controlled tautomerism of **DPH_{22}** has been successfully used for the construction of an integrated molecular level half-subtractor and comparator. In addition, this acid/base-switched tautomerism is reversible, thus endowing the system with ease of reset and recycling; consequently, there is no need to modulate complicated intermolecular interactions and electron-/charge-transfer processes.

Introduction

As the development of increasingly minute semiconductor computation devices is approaching its physical limits, a large variety of molecular systems and chemical reactions offer a potential strategy for computation at the molecular level.[1] Since the initial report of the AND gate,[2] a variety of molecular logic gates, including AND, OR, NOT, XOR, XNOR, NAND, and INH, have been reported.[3] Molecular logic circuits that use a combination of these logic gates can be applied to realize information processing based on the Boolean logic of elementary computations by using several different inputs.[4] In fact, similar molecular-level processing in solvated media continuously occurs in living systems in which enzyme-based logics and DNA encoding operate.[5] To realize multiple arithmetical operations, it is essential to develop molecules or supramolecular systems with multiple stable states that can be interconverted reversibly by applying simple inputs.[6] Although rich opportunities are offered by supramolecular assemblies, the construction and modulation of complicated intermolecular interactions are required. In contrast, the use of discrete molecular entities may avoid these difficulties if suitable molecular structures can be developed.[7]

Tautomerism is one of the most commonly used means of generating multiple stable states based on a unimolecular platform.[8] In the realm of porphyrin chemistry, N–H tautomerism usually occurs by means of proton transfer among the nitrogen atoms at the porphyrin core or at the periphery in N-confused porphyrins.[9] In these cases, it is difficult to discriminate the possible tautomers because the proton-transfer processes are too fast to be monitored at room temperature, thus limiting their applications as logic devices. Also, tautomeric processes lack complexity in simple symmetrical oxoporphyrinogens.[10] The generation of multiple stable states within a single porphyrinoid remains challenging. Herein, we have designed and prepared the unsymmetrical macrocycle dioxoporphyrin **DPH_{22}**, thus making a breakthrough in the stepwise modulation of tautomerization, protonation, and deprotonation processes to lead to the construction of novel multifunctional molecular devices based on multiple stable states.

Dioxoporphyrin **DPH_{22}** (Scheme 1) has two basic tautomeric states, namely, the phenolic form **DPH_{22}** and the quinoidal form **DPH_{40}**. In the **DPH_{mn}** notation, the subscripts *m* and *n* denote the respective numbers of NH and OH protons. Surprisingly, **DPH_{22}** undergoes quantitative tautomeric conversion from the phenolic state into the quinoidal state upon the addition of dimethylsulphoxide (DMSO), H^+ ions, or F^- ions in solu-

[a] Dr. Y. Ding, Prof. Dr. W. Zhu, Prof. Dr. H. Tian, Prof. Dr. Y. Xie
Key Laboratory for Advanced Materials and Institute of Fine Chemicals
Shanghai Key Laboratory of Functional Materials Chemistry
East China University of Science and Technology
Shanghai 200237 (P.R. China)
Fax: (+86) 21-6425-2758
E-mail: yshxie@ecust.edu.cn

[b] Dr. X. Li, Prof. Dr. H. Ågren
Division of Theoretical Chemistry and Biology
School of Biotechnology, KTH Royal Institute of Technology
10691 Stockholm (Sweden)

[c] Dr. J. P. Hill, Prof. Dr. K. Ariga
WPI-Center for Materials Nanoarchitectonics
National Institute for Materials Science (NIMS)
Namiki 1-1, Tsukuba, Ibaraki (Japan)

[d] Prof. Dr. J. Andréasson
Department of Chemical and Biological Engineering
Physical Chemistry, Chalmers University of Technology
412 96 Göteborg (Sweden)

Supporting information for this article is available on the WWW under http://dx.doi.org/10.1002/chem.201403830.

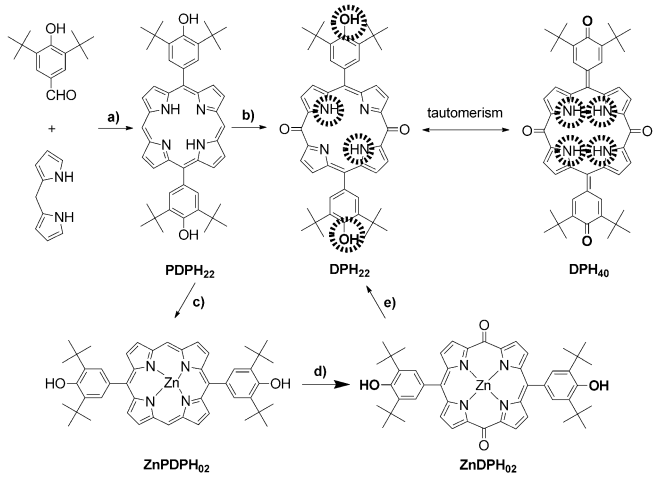

Scheme 1. Preparation of dioxoporphyrin **DPH_{22}** and the chemical structure of the tautomer **DPH_{40}**. Reaction conditions: a) 1) TFA, CH_2Cl_2; 2) DDQ; b) $Tl(CF_3COO)_3$, TFA, CH_2Cl_2; c) $Zn(OAc)_2{\cdot}2H_2O$, $CHCl_3$, MeOH; d) $FeCl_3$, DMF, reflux; e) H_2SO_4, $CHCl_3$. DDQ = 2,3-dichloro-5,6-dicyano-1,4-benzoquinone.

tion with $CHCl_3$. Furthermore, the alternate addition of H^+ and F^- ions reversibly switches the tautomerism between the phenolic and quinoidal forms accompanied by protonation/deprotonation processes and conformational changes. By using H^+ and F^- ions as the inputs and absorption variations as the outputs, it proved feasible to construct and combine two half-subtractors and a comparator to perform binary subtraction operations.

Results and Discussion

Synthesis, characterization, and solvent-triggered tautomerism of porphyrinoid DPH_{22}

Compound **DPH_{22}** was synthesized by two different routes and has been fully characterized (see Scheme 1 and Figures S1–S8 in the Supporting Information). The first synthesis entails the direct oxidation of porphyrin **$PDPH_{22}$** by using $(CF_3COO)_3Tl$ (TTFA)[11] in CH_2Cl_2/trifluoroacetic acid (TFA) in a yield of 62%. In spite of the mild reaction conditions and the satisfactory yield, the high toxicity of thallium urged us to explore alternative synthetic routes. Thus, **$PDPH_{22}$** was first complexed with zinc(II) to afford **$ZnPDPH_{02}$**, which could then be oxidized to **$ZnDPH_{02}$** with anhydrous $FeCl_3$[12] in DMF heated to reflux. Demetallation of **$ZnDPH_{02}$** with H_2SO_4 gave **DPH_{22}** in an overall yield of approximately 35%. Interestingly, during the purification of **DPH_{22}**, the addition of polar solvents such as DMF and DMSO to solutions of **DPH_{22}** in CH_2Cl_2 or $CHCl_3$ drastically changed the solution color from light yellow to deep purple. Indeed, pronounced UV/Vis absorption spectral changes could also be observed during the addition of DMF or DMSO to a solution of **DPH_{22}** in $CHCl_3$, for which the peak at $\lambda = 412$ nm was attenuated and a new broad peak appeared at approximately $\lambda = 560$ nm (see Figure S9 in the Supporting Information). Isosbestic points were observed, which are indicative of the formation of a well-defined new species, due to tautomerization. To obtain further insight into the nature of the transformation, ^1H NMR spectral changes of **DPH_{22}** in $CDCl_3$ during titration with $[D_6]$DMSO were observed (see Figure S10 in the Supporting Information). In the spectra, **DPH_{22}** initially contains peaks due to two inner NH protons (at $\delta = 14.00$ ppm) and two phenolic OH hydrogen atoms (at $\delta = 5.54$ ppm). These peaks gradually decrease in intensity upon increasing addition of $[D_6]$DMSO. An aliquot of $[D_6]$DMSO (1.0 μL) was required for 100% conversion into a set of peaks that correspond to the quinoidal form of **DPH_{40}**, with four NH hydrogen atoms (at $\delta =$ 11.65 ppm) and no peak for OH. Thus, the addition of DMSO induced a well-defined tautomeric transformation of **DPH_{22}** from the phenolic form to the quinoidal form. To understand this behavior further, we calculated the optimized geometries (see Figure S11 in the Supporting Information) and the corresponding free energies of **DPH_{22}**, **DPH_{40}**, and another possible tautomer **DPH_{22}-A** in various solvents (see Figure 1 and

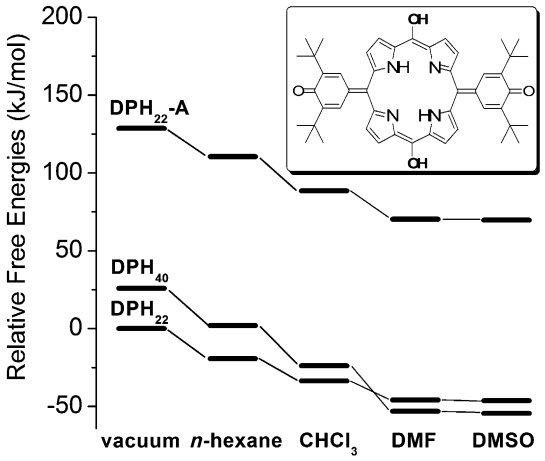

Figure 1. Relative free energies (in $kJ\,mol^{-1}$) of **DPH_{22}**, **DPH_{40}**, and **DPH_{22}-A**, with respect to **DPH_{22}** in vacuum. Inset: molecular structure of **DPH_{22}-A**.

Table S1 in the Supporting Information). The calculations suggest that the free energies of **DPH_{22}** are lower than those of **DPH_{40}** in less-polar solvents, whereas the values in more-polar solvents are reversed. More specifically, the energy of **DPH_{22}** in $CHCl_3$ is 9.8 $kJ\,mol^{-1}$ lower than that of **DPH_{40}**. In contrast, the energy of **DPH_{22}** in DMSO is 8.2 $kJ\,mol^{-1}$ higher than that of **DPH_{40}**. Hence, it can be anticipated that almost quantitative conversion from **DPH_{22}** into **DPH_{40}** would be observed when the solvent is changed from $CHCl_3$ to DMSO, which is consistent with the results of the NMR spectroscopic analysis. The energies for **DPH_{22}-A** are significantly higher than those for the other two tautomers in all the cases. Therefore, it was not observed at all.

To obtain further insight into the molecular structures of **DPH_{22}** and **DPH_{40}**, we performed crystallizations from different solvents according to the abovementioned solvent-triggered tautomerism behavior. Fortunately, single crystals of **DPH_{22}** and **$DPH_{40}{\cdot}2$ DMF** were obtained from mixtures of $CHCl_3$/*n*-octane

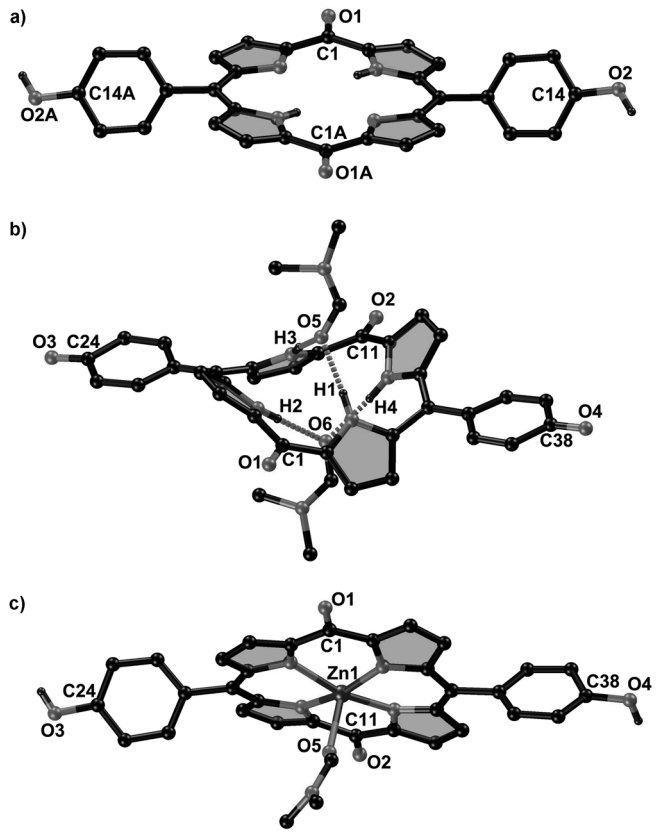

Figure 2. X-ray crystal structures of a) **DPH_{22}**, b) **DPH_{40}·2 DMF**, and c) **$ZnDPH_{02}$·3 DMF**. The *tert*-butyl groups and hydrogen atoms attached to the carbon atoms have been omitted for clarity.

and DMF/H_2O, respectively.[13] Compound **DPH_{22}** is nearly planar (Figure 2a), with bond lengths C1–O1 and C14–O2 (1.243(6) and 1.364(5) Å, respectively) that indicate a C=O double bond and a C–O single bond, respectively; consequently, these data are consistent with its assignment as the phenolic tautomer. In contrast, **DPH_{40}·2 DMF** is severely distorted due to steric hindrance at the four inner NH hydrogen atoms (Figure 2b). The four pyrrolic units in **DPH_{40}·2 DMF** are arranged in a saddlelike conformation, with two DMF molecules hydrogen bonded to the inner NH hydrogen atoms from both sides of the macrocycle (H3···O5 and H1···O5 distances of 2.01 and 1.98 Å and H2···O6 and H4···O6 distances of 2.04 and 1.94 Å, respectively). In addition, the C1–O1, C11–O2, C24–O3, and C38–O4 bond lengths in **DPH_{40}·2 DMF** all lie in the range 1.232(4)–1.233(4) Å, thus indicating C=O double bonds.[10c]

The Zn^{2+} complex of **DPH_{22}** was also successfully crystallized from DMF. For **$ZnDPH_{02}$·3 DMF** (Figure 2c), phenolic C–O single bonds are present with the bond lengths[12] of 1.364(5) and 1.385(5) Å, respectively. This finding indicates that planar **DPH_{22}** can coordinate as a dianionic ligand with two NH moieties coordinated in their deprotonated form.

F^-- and H^+-induced tautomerism

The presence of hydrogen bonds in the crystal of **DPH_{40}·2 DMF** indicates that the conversion from **DPH_{22}** into **DPH_{40}** may be promoted by strong hydrogen bonding with polar solvents,[14] which is a feature that is in accordance with the solvent-triggered tautomerism observed by ^{1}H NMR and UV/Vis spectroscopic measurements. The F^- ion is also a strong proton acceptor for hydrogen bonding; hence, a solution of **DPH_{22}** in $CHCl_3$ was titrated with F^- ions. Interestingly, two distinct sets of isosbestic points were observed. Initially, the addition of approximately 0–9 equivalents of F^- ions induced a tautomeric shift from **DPH_{22}** to **$DPH_{40}F^-$**, with a concomitant decrease of the absorption band at $\lambda = 412$ nm and the development of a broad band centered at $\lambda = 552$ nm, with one set of isosbestic points (Scheme 2 and Figure 3a). Further addition of approximately 10–50 equivalents of F^- ions induced the deprotonation[14] of **DPH_{40}** to **DPH_{20}^{2-}** (see Scheme 2, Figure 3b, and Tables S2 and S3 in the Supporting Information) with a concomitant decrease of the absorption band at $\lambda = 552$ nm and development of a broad peak centered at $\lambda = 700$ nm with a new set of isosbestic points. In contrast, when the titration of F^- ions was carried out in DMSO, only the deprotonation process could be observed (see Figure S12 in the Supporting Information), which is ascribed to the fact that the compound already exists in the **DPH_{40}** form in DMSO (**DPH_{22}** exists in $CHCl_3$).

DPH_{22} contains two imino nitrogen atoms, which may be readily protonated, thus resulting in the distortion of the macrocycle from a planar conformation due to steric hindrance between the NH hydrogen atoms and therefore might induce a tautomeric shift to the quinoidal form. Consistent with these expectations, the addition of approximately 0–4.4 equivalents of TFA to a solution of **DPH_{22}** in $CHCl_3$ caused absorption changes similar to those induced by the addition of DMSO (Figure 3c). Upon the addition of 3.0 equivalents of TFA to a solution of **DPH_{22}** in $CDCl_3$, the ^{1}H NMR spectrum shows peaks similar to those of **DPH_{40}**, except that two additional hydrogen atoms are observed at $\delta = 6.49$ ppm (see Figure S13 in the Supporting Information), which can be assigned to those attached to the quinoidal oxygen atoms in the **DPH_{42}^{2+}** ion

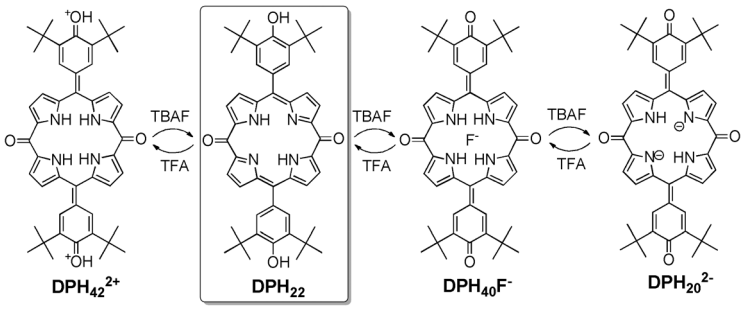

Scheme 2. Schematic representation of TBAF/TFA-induced tautomeric variation of **DPH_{22}** in $CHCl_3$.

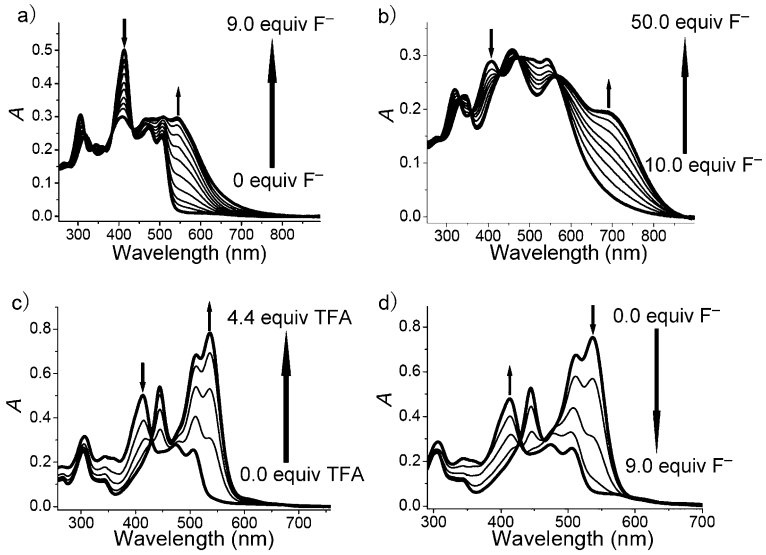

Figure 3. UV/Vis spectral changes during the titration of **DPH_{22}** (10 μM) with TBAF and TFA in $CHCl_3$: a) 0–9.0 and b) 10.0–50.0 equivalents of TBAF, c) 0–4.4 equivalents of TFA, and d) 0–9.0 equivalents of TBAF.

(Scheme 2). The proposed structure for the **DPH_{42}^{2+}** ion was supported by DFT calculations (see Figures S14 and S15 and Table S4 in the Supporting Information). In summary, the addition of TFA induces the simultaneous protonation and tautomerism of **DPH_{22}**, thus affording the **DPH_{42}^{2+}** ion.

Reversible tautomerism controlled by the addition of TFA and TBAF

Considering the fact that TFA and tetrabutylammonium fluoride (TBAF) can neutralize the effect of each other, and that the addition of either TFA or TBAF causes tautomerism from the phenolic to the quinoidal form, it was anticipated that the alternate addition of TFA and TBAF would reversibly switch the tautomerization between the phenolic and the quinoidal states. Accordingly, the addition of TBAF to a solution of the **DPH_{42}^{2+}** ion regenerated the absorption peaks of **DPH_{22}** (Figure 3d). The addition of TFA to the **DPH_{20}^{2-}** ion also regenerates **DPH_{22}**. Thus, **DPH_{22}** can be reversibly switched between the phenolic form **DPH_{22}** and the quinoidal forms **DPH_{42}^{2+}**, **$DPH_{40}F^{-}$**, and **DPH_{20}^{2-}** through the controlled addition of TFA and TBAF (see Scheme 2 and Figure S16 in the Supporting Information).

Integrated operation of a digital comparator and two half-subtractors

Based on this reversible tautomeric switching, two half-subtractors and a digital comparator were constructed for the purpose of realizing a subtraction process. The addition of TFA and TBAF were defined as $input_1$ (In_1) and $input_2$ (In_2), respectively. UV/Vis absorption at $\lambda = 412$, 510, 562, and 603 nm was defined as $output_1$-$output_4$ (out_1-out_4). The input-dependent absorption spectra in $CHCl_3$ are shown in Figure 4. In the absence or simultaneous presence of In_1 and In_2 (Figure 4, lines A and D), **DPH_{22}** exists in its original form with an absorption peak at $\lambda = 412$ nm. With only In_1 (Figure 4, line B), **DPH_{22}** is protonated to its **DPH_{42}^{2+}** form and sharp absorption changes are observed with new absorption peaks at $\lambda = 441$, 510, and 535 nm and decreased absorption at $\lambda = 412$ nm. In the presence of In_2 only (Figure 4, line C), hydrogen-bonding-induced tautomerism also leads to significant absorption changes with the development of a broad peak centered at about $\lambda = 560$ nm. Hence, according to these absorption changes, threshold values can be set at 0.35, 0.35, 0.12, and 0.12 for the absorption at $\lambda = 412$, 510, 562, and 603 nm, respectively. When no or both inputs are applied, absorption at $\lambda = 412$ nm exceeds the threshold, and the observed out_1 is 1; therefore, out_1 performs as an XNOR gate. Similarly, out_2 and out_4 can be considered to act as INH gates and out_3 can act as an XOR gate.

It is noteworthy that, in this case, all four logic gates share the same inputs but can be operated independently without mutual interference. Combined operation of the two INH gates at $\lambda = 510$ and 603 nm with the XOR gate at $\lambda = 562$ nm generates two half-subtractors. Also, a comparator can be constructed by combining the INH gate at $\lambda = 510$ nm and the XNOR gate at $\lambda = 412$ nm. The corresponding electronic symbols and truth tables are shown in Figure S17 and Table S5 (see the Supporting Information). On the basis of these results, integrated operation of the digital comparator with the two half-subtractors can be used to perform binary subtraction operations based on the following considerations: the comparator decides the relative magnitude between the two inputs before selecting the half-subtractor to carry out the subtraction to generate a positive subtraction value.

Conclusion

A novel dioxoporphyrin **DPH_{22}** has been synthesized and the tautomerism between its phenolic and quinoidal states could be controlled by varying solvents or the addition of H^+ and F^- ions, with both tautomers successfully characterized by X-ray crystallographic studies. This readily modulated tautomerism could be usefully applied to the construction of molecular devices. Thus, two half-subtractors and a comparator were successfully developed. Furthermore, integrated operations of the half-subtractors and the comparator improved the feasibility of the subtraction process. Compared with the majority of the reported logic devices based on supramolecular systems, our porphyrinoid-based system avoids some challenging construction requirements; therefore, there is no need to modulate complicated intermolecular interactions or energy/electron-transfer processes.[15] In addition, our acid/base-switched tautomerism is reversible, thus endowing the system with ease of reset and recycling. In conclusion, in contrast to the commonly observed N–H tautomerism among the nitrogen atoms of normal porphyrins, which is too fast to be monitored at room

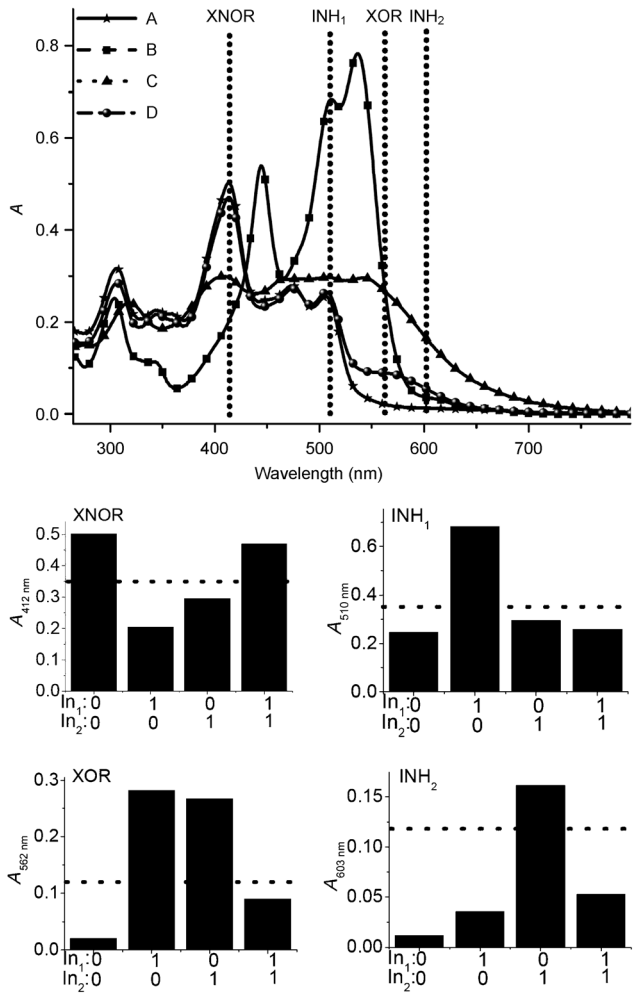

Figure 4. Top: Absorption spectra of the relevant tautomeric forms (total concentration = 10 μM) in $CHCl_3$ under various conditions. Line A) In the absence of In_1 and In_2, B) only In_1, C) only In_2, D) $In_1 + In_2$. Below: Four experimental outputs for the XNOR, INH, XOR, and INH gates observed at $\lambda = 412$, 510, 562, and 603 nm, respectively, under the same input conditions. Dotted lines indicate the threshold values. In_1: 4.4 equivalents of TFA (H^+); In_2: 9.0 equivalents of TBAF (F^-).

temperature, our conformational transformation approach based on a novel dioxoporphyrin **DPH_{22}** enables the generation of stable states that even can be fully characterized by X-ray crystallographic studies. We have provided an attractive, efficient, and step-by-step approach to modulate the tautomerization, protonation, and deprotonation processes to construct logic devices useful for binary calculations by using a single porphyrinoid compound.

Experimental Section

General

Commercially available solvents and reagents were used as received. Deuterated solvents for the NMR spectroscopic measurements were available from Aldrich. UV/Vis absorption spectra were recorded on a Varian Cary 100 spectrophotometer, with a quartz cuvette (path length = 1 cm). ^{1}H NMR spectra were obtained by using a Bruker AM400 spectrometer with TMS as an internal standard. High-resolution mass spectra were measured on a Waters LCT Premier XE spectrometer. Column chromatography was carried out without special precautions to exclude air on silica gel (200–300 mesh). Reactions were monitored by using TLC analysis.

UV/Vis absorption spectrum measurements

The absorption spectra of **DPH_{22}** (10 μM) were measured at 25 °C in $CHCl_3$. The tested acid and base were added as trifluoroacetic acid (TFA) and tetrabutylammonium fluoride (TBAF) dissolved in $CHCl_3$.

Synthesis of $PDPH_{22}$: 3,5-Di(*tert*-butyl)-4-hydroxybenzaldehyde (1.49 g, 6.4 mmol) and 2,2′-dipyrrolylmethane (932 mg, 6.4 mmol) were dissolved in CH_2Cl_2 (1.5 L) in a 2 L round-bottom flask under nitrogen. TFA (190 μL) was added to the solution, which was stirred in the dark at room temperature for 2.5 h. DDQ (2.12 g, 9.3 mmol) was added to the reaction mixture and stirring continued for approximately 1–2 min, followed by the addition of triethylamine (1 mL). The solvent was removed under reduced pressure and the crude product was purified by flash chromatography on silica gel (200–300 mesh) to afford **$PDPH_{22}$** (517 mg, 22.5%). ^{1}H NMR ($CDCl_3$, 400 MHz, 298 K): $\delta = 10.29$ (s, 2H; *meso*-CH), 9.40 (d, $J = 4.8$ Hz, 4H; pyrrolic-βH), 9.17 (d, $J = 4.8$ Hz, 4H; pyrrolic-βH), 8.11 (s, 4H; phenyl), 5.59 (s, 2H; phenyl-OH), 1.68 (s, 36H; $C(CH_3)_3$), −2.96 ppm (2H; inner NH); HRMS: *m/z* calcd for $C_{48}H_{55}N_4O_2$ $[M+H^+]$: 719.4325: found: 719.4325.

Synthesis of $ZnPDPH_{02}$: **$PDPH_{22}$** (380 mg, 0.53 mmol) and $Zn(OAc)_2 \cdot 2H_2O$ (231 mg, 1.05 mmol) were dissolved in a mixture of $CHCl_3$ (137 mL) and MeOH (63 mL), and the resulting solution was stirred at 40 °C for 1 h. After removal of the solvents under reduced pressure, the crude product was purified by flash chromatography on silica gel (200–300 mesh) and washed with MeOH to afford **$ZnPDPH_{02}$** (392 mg, 95%). ^{1}H NMR ($CDCl_3$, 400 MHz, 298 K): $\delta =$ 10.31 (s, 2H; *meso*-CH), 9.45 (d, $J = 4.8$ Hz, 4H; pyrrolic-βH), 9.23 (d, $J = 4.4$ Hz, 4H; pyrrolic-βH), 8.10 (s, 4H; phenyl), 5.56 (s, 2H; phenyl-OH), 1.67 ppm (s, 36H; $C(CH_3)_3$).

Synthesis of DPH_{22}

Route 1: Porphyrin **$PDPH_{22}$** (80 mg, 0.11 mmol) was dissolved in a mixture of TFA (3 mL) and CH_2Cl_2 (16 mL) with stirring, followed by slowly adding a solution of thallium(III) trifluoroacetate (1.1 g, 2 mmol) in TFA (3 mL). The resulting mixture was stirred at room temperature for 30 min and then poured into water (130 mL). The mixture was extracted with CH_2Cl_2, the organic phase dried over anhydrous Na_2SO_4, and the solvents removed under reduced pressure. Demetallization of the residue was carried out immediately by stirring in TFA (3 mL) for 2 h, followed by washing with water and extraction with CH_2Cl_2. Removal of solvents under reduced pressure yielded the crude product, which was purified by chromatography on silica gel (eluent: CH_2Cl_2) to afford **DPH_{22}** (52 mg, 62.4%). ^{1}H NMR ($CDCl_3$, 400 MHz, 298 K): $\delta = 14.00$ (s, 2H; NH), 7.25 (s, 4H; Ph-H), 7.21 (d, $J = 4.4$ Hz, 4H; pyrrolic-βH), 6.64 (br, 4H; pyrrolic-βH), 5.54 (s, 2H; OH), 1.48 ppm (s, 36H; $C(CH_3)_3$). Quinoidal tautomer **DPH_{40}**: ^{1}H NMR ($CDCl_3 + [D_6]$DMSO, 400 MHz, 298 K): $\delta =$ 11.65 (s, 4H; NH), 7.53 (s, 4H; Ph-H), 7.21 (s, 4H; pyrrolic-βH), 6.75 (s, 4H; pyrrolic-βH), 1.33 ppm (s, 36H; $C(CH_3)_3$); HRMS: *m/z* calcd for $C_{48}H_{53}N_4O_4$ $[M+H^+]$: 749.4067; found: 749.4073.

Route 2: **$ZnPDPH_{02}$** (39 mg, 0.05 mmol) and anhydrous $FeCl_3$ (82 mg, 0.5 mmol) were dissolved in DMF (15 mL) and heated to reflux for 5 h. The DMF was removed under reduced pressure. The resulting solid was dissolved in a mixture of $CHCl_3$ (30 mL) and

H_2SO_4 (10 mL), vigorously stirred for 1 h, and washed with water. After the solvent was removed under reduced pressure, the crude product was purified by chromatography on silica gel (eluent: CH_2Cl_2) to afford **DPH_{22}** (13 mg, 35%).

Synthesis of $ZnDPH_{02}$: **DPH_{22}** (90 mg, 0.12 mmol) and $Zn(OAc)_2{\cdot}2H_2O$ (106 mg, 0.48 mmol) were dissolved in a mixture of $CHCl_3$ (60 mL), MeOH (15 mL), and DMSO (1 mL), and the solution was stirred at 40 °C for 2 h. After removing the solvents under reduced pressure, the crude product was purified by flash chromatography on silica gel (200–300 mesh) to afford **$ZnDPH_{02}$** (89 mg, 89.7%). ^{1}H NMR ($CDCl_3$, 400 MHz, 298 K) $\delta = 7.21$ (s, 4H; phenyl), 7.12 (t, 4H; pyrrolic-βH), 6.60 (d, $J = 4.4$ *Hz*, 4H; pyrrolic-βH), 5.63 (s, 2H; phenyl-OH), 1.47 ppm (s, 36H; $C(CH_3)_3$); HRMS: *m/z* calcd for $C_{48}H_{51}N_4O_4Zn_1$ $[M+H^+]$: 811.3202; found: 811.3201.

Crystallography

Single crystals of **DPH_{22}** suitable for X-ray analysis were grown by slow evaporation of its solution in a mixture of $CHCl_3$ and *n*-octane. Single crystals of **DPH_{40}·2 DMF** and **$ZnDPH_{02}$·3 DMF** were grown by slow diffusion of H_2O vapor into their corresponding DMF solutions.

Crystal data for [DPH_{22}]: $C_{48}H_{52}N_4O_4$, $M_w = 748.94$ g mol^{-1}, $0.38\times0.27\times0.24$ mm^3, monoclinic, $P21/c$, $a = 6.2320(5)$, $b = 18.2401(16)$, $c = 19.1359(18)$ Å, $\beta = 105.8410(10)^\circ$, $V = 2092.6(3)$ Å^3, $F(000) = 800$, $\rho_{calcd} = 1.189$ Mg·m^{-3}, μ(MoKα) = 0.076 mm^{-1}, $T = 298(2)$ K, 10234 data were measured on a Bruker SMART Apex diffractometer, of which 3669 were unique ($R_{int} = 0.1422$); 259 parameters were refined against Fo^2 (all data), final $wR_2 = 0.1738$, $S = 1.026$, R_1 ($I > 2\sigma(I)$) = 0.0872, largest final difference peak/hole = +0.280 and −0.252 e Å^{-3}. Structure solution by using direct methods and full-matrix least-squares refinement against F^2 (all data) with SHELXTL.

Crystal data for [DPH_{40}·2 DMF]: $C_{54}H_{66}N_6O_6$, $M_w = 895.13$ g mol^{-1}, $0.20\times0.10\times0.02$ mm^3, monoclinic, $C2/c$, $a = 41.6159(15)$, $b = 9.7166(4)$, $c = 29.1881(12)$ Å, $\beta = 91.106(3)^\circ$, $V = 11\,800.4(8)$ Å^3, $F(000) = 3840$, $\rho_{calcd} = 1.008$ Mg·m^{-3}, μ(MoKα) = 0.526 mm^{-1}, $T = 298(2)$ K, 26828 data were measured on a Bruker SMART Apex diffractometer, of which 9590 were unique ($R_{int} = 0.0381$); 611 parameters were refined against Fo^2 (all data), final $wR_2 = 0.2288$, $S = 1.057$, R_1 ($I > 2\sigma(I)$) = 0.0775, largest final difference peak/hole = +1.262 and −0.471 e Å^{-3}. Structure solution by using direct methods and full-matrix least-squares refinement against F^2 (all data) with SHELXTL.

Crystal data for [$ZnDPH_{02}$·3 DMF]: $C_{57}H_{71}N_7O_7Zn$, $M_w = 1031.58$ g mol^{-1}, $0.50\times0.21\times0.20$ mm^3, triclinic, P-1, $a = 14.0420(13)$, $b = 14.9580(14)$, $c = 15.5440(15)$ Å, $\alpha = 62.1320(10)$, $\beta = 73.990(2)$, $\gamma = 75.328(2)^\circ$, $V = 2744.4(4)$ Å^3, $F(000) = 1096$, $\rho_{calcd} = 1.248$ Mg·m^{-3}, μ(MoKα) = 0.505 mm^{-1}, $T = 298(2)$ K, 13790 data were measured on a Bruker SMART Apex diffractometer, of which 9527 were unique ($R_{int} = 0.0305$); 727 parameters were refined against Fo^2 (all data), final $wR_2 = 0.1687$, $S = 1.069$, R_1 ($I > 2\sigma(I)$) = 0.0666, largest final difference peak/hole = +0.760 and −1.090 e Å^{-3}. Structure solution by using direct methods and full-matrix least-squares refinement against F^2 (all data) with SHELXTL.

Computational details and DFT-calculation results

We employed DFT calculations to study compounds **DPH_{22}**, **DPH_{42}^{2+}**, and their isomers. The ground-state geometries and frontier molecular orbitals of the compounds were computed by using the hybrid B3LYP functional[16] and the Pople 6–31G* basis set,[17] with solvent effects taken into account by the polarizable-continuum model.[18] Frequency analyses were conducted to ensure that the optimized geometries are true minima. Frequency analyses also provide Gibbs free energies at ambient temperature as the sum of the self-consistent field (SCF) energy, zero-point correction, and thermal correction. All the calculations were carried out by using the Gaussian 09 program package.[19] Table S1 summarizes the relative free energies (in kJ mol^{-1}) of **DPH_{22}**, **DPH_{40}**, and **DPH_{22}-A**, with respect to **DPH_{22}** in a vacuum (see the Supporting Information).

Calculations of the deprotonation of DPH_{40} with F^- ions (Scheme S1)

The energies of the compounds were computed at the B3LYP/6–31G* level of theory and are shown in Tables S2 and S3 (see the Supporting Information). The overall free-energy change of the deprotonation process of **DPH_{40}** to **DPH_{30}^-** is −59.2 kcal mol^{-1}, thus indicating that **DPH_{40}** can be easily deprotonated to the **DPH_{30}^-** form. Further calculation reveals that the deprotonation of **DPH_{30}^-** to **DPH_{20}^{2-}** is also thermodynamically favorable, with a free-energy change of −45.6 kcal mol^{-1}.

Calculations of the structure of DPH_{42}^{2+} ions (Scheme S2 in the Supporting Information)

It has been demonstrated by ^{1}H NMR and UV/Vis spectroscopic measurements that the protonated structure of **DPH_{22}** is in the quinoidal form, but there are two possible structures (as shown in Scheme S2 in the Supporting Information), named as **DPH_{42}^{2+}** and **DPH_{42}^{2+}-A**. Theoretical computations suggest that **DPH_{42}^{2+}-A** has a much larger free energy than the **DPH_{42}^{2+}** isomer in $CHCl_3$ (see Figure S14 and Table S4 in the Supporting Information). This value is related to the dihedral angle γ between the phenyl/quinone group and the porphyrin ring and the distance between the two hydrogen atoms at the a and b sites in **DPH_{42}^{2+}** and **DPH_{42}^{2+}-A**. The dihedral angle γ in **DPH_{42}^{2+}** is larger than that of **DPH_{42}^{2+}-A** owing to the fact that the C–C bond in **DPH_{42}^{2+}** at the *meso* site of the porphyrin ring shows a stronger single bond character (compare the C–C bond lengths for **DPH_{22}** and **DPH_{40}** in Figure S15 in the Supporting Information) and that the quinone group shows a stronger aromatic character (see the HOMO in Figure S15) after the protonation at the quinone oxygen site. Moreover, the distance between H_a and H_b is larger in **DPH_{42}^{2+}** (Table S4), which is indicative of a less sterically hindered geometry.

Acknowledgements

This work was financially supported by NSFC (21072060, 91227201), the Oriental Scholarship, NCET-11–0638, and the Fundamental Research Funds for the Central Universities (WK1013002).

Keywords: half-subtractors · logic gates · organic electronics · porphyrinoids · tautomerism

[1] a) P. Ball, *Nature* **2000**, *406*, 118–120; b) A. P. de Silva, S. Uchiyama, *Nat. Nanotechnol.* **2007**, *2*, 399–410; c) T. Carell, *Nature* **2011**, *469*, 45–46; d) A. Credi, *Angew. Chem.* **2007**, *119*, 5568–5572; *Angew. Chem. Int. Ed.* **2007**, *46*, 5472–5475.

[2] A. P. de Silva, N. H. Q. Gunaratne, C. P. McCoy, *Nature* **1993**, *364*, 42–44.

[3] a) S. Bi, B. Ji, Z. Zhang, J.-J. Zhu, *Chem. Sci.* **2013**, *4*, 1858–1863; b) K. S. Park, M. W. Seo, C. Jung, J. Y. Lee, H. G. Park, *Small* **2012**, *8*, 2203–2212; c) Y. Liu, A. Offenhäusser, D. Mayer, *Angew. Chem.* **2010**, *122*, 2649–

2652; *Angew. Chem. Int. Ed.* **2010**, *49*, 2595 – 2598; d) K. Szaciłowski, *Chem. Rev.* **2008**, *108*, 3481 – 3548; e) S. Ozlem, E. U. Akkaya, *J. Am. Chem. Soc.* **2008**, *130*, 48 – 49; f) D. H. Qu, F. Y. Ji, Q. C. Wang, H. Tian, *Adv. Mater.* **2006**, *18*, 2035 – 2038; g) S. D. Straight, J. Andréasson, G. Kodis, S. Bandyopadhyay, R. H. Mitchell, T. A. Moore, A. L. Moore, D. Gust, *J. Am. Chem. Soc.* **2005**, *127*, 9403 – 9409; h) D. Karak, S. Das, S. Lohar, A. Banerjee, A. Sahana, I. Hauli, S. K. Mukhopadhyay, D. A. Safin, M. G. Babashkina, M. Bolte, Y. Garcia, D. Das, *Dalton Trans.* **2013**, *42*, 6708 – 6715; i) D. S. Kim, V. M. Lynch, J. S. Park, J. L. Sessler, *J. Am. Chem. Soc.* **2013**, *135*, 14889 – 14894.

[4] a) M. Kumar, N. Kumar, V. Bhalla, *Chem. Commun.* **2013**, *49*, 877 – 879; b) Y. Zhang, L. Lei, J. J. Dong, X. L. Zhang, *Optics Commun.* **2012**, *285*, 407 – 411; c) T. Nishimura, Y. Ogura, J. Tanida, *Appl. Phys. Lett.* **2012**, *101*, 233703 – 233704; d) V. Luxami, S. Kumar, *Dalton Trans.* **2012**, *41*, 4588 – 4593; e) J. Andréasson, U. Pischel, S. D. Straight, T. A. Moore, A. L. Moore, D. Gust, *J. Am. Chem. Soc.* **2011**, *133*, 11641 – 11648; f) S. J. Langford, T. Yann, *J. Am. Chem. Soc.* **2003**, *125*, 11198 – 11199; g) D. Margulies, G. Melman, C. E. Felder, R. Arad-Yellin, A. Shanzer, *J. Am. Chem. Soc.* **2004**, *126*, 15400 – 15401; h) D. Margulies, C. E. Felder, G. Melman, A. Shanzer, *J. Am. Chem. Soc.* **2006**, *128*, 347 – 354.

[5] a) L. Adleman, *Science* **1994**, *266*, 1021 – 1024; b) Q. Jiang, Z. G. Wang, B. Q. Ding, *Small* **2013**, *9*, 1016 – 1020; c) C. N. Yang, C. Y. Hsu, Y. C. Chuang, *Chem. Commun.* **2012**, *48*, 112 – 114; d) J. Elbaz, F. A. Wang, F. Remacle, I. Willner, *Nano Lett.* **2012**, *12*, 6049 – 6054; e) E. Katz, V. Privman, *Chem. Soc. Rev.* **2010**, *39*, 1835 – 1857; f) T. Li, E. Wang, S. Dong, *J. Am. Chem. Soc.* **2009**, *131*, 15082 – 15083; g) R. Gaber, T. Lebar, A. Majerle, B. Šter, A. Dobnikar, M. Benčina, R. Jerala, *Nat. Chem. Biol.* **2014**, *10*, 203 – 208.

[6] a) J. Andreasson, S. D. Straight, S. Bandyopadhyay, R. H. Mitchell, T. A. Moore, A. L. Moore, D. Gust, *Angew. Chem.* **2007**, *119*, 976 – 979; *Angew. Chem. Int. Ed.* **2007**, *46*, 958 – 961; b) D. Margulies, G. Melman, A. Shanzer, *J. Am. Chem. Soc.* **2006**, *128*, 4865 – 4871; c) G. de Ruiter, M. E. van der Boom, *Angew. Chem.* **2012**, *124*, 8726 – 8729; *Angew. Chem. Int. Ed.* **2012**, *51*, 8598 – 8601; d) T. Gupta, M. E. van der Boom, *Angew. Chem.* **2008**, *120*, 5402 – 5406; *Angew. Chem. Int. Ed.* **2008**, *47*, 5322 – 5326.

[7] a) J. Kärnbratt, M. Hammarson, S. M. Li, H. L. Anderson, B. Albinsson, J. Andreasson, *Angew. Chem.* **2010**, *122*, 1898 – 1901; *Angew. Chem. Int. Ed.* **2010**, *49*, 1854 – 1857; b) K. S. Hettie, J. L. Klockow, T. E. Glass, *J. Am. Chem. Soc.* **2014**, *136*, 4877 – 4880; c) P. Ceroni, G. Bergamini, V. Balzani, *Angew. Chem.* **2009**, *121*, 8668 – 8670; *Angew. Chem. Int. Ed.* **2009**, *48*, 8516 – 8518; d) W. Sun, C. Zhou, C.-H. Xu, C.-J. Fang, C. Zhang, Z.-X. Li, C.-H. Yan, *Chem. Eur. J.* **2008**, *14*, 6342 – 6351; e) U. Pischel, *Angew. Chem.* **2007**, *119*, 4100 – 4115; *Angew. Chem. Int. Ed.* **2007**, *46*, 4026 – 4040.

[8] a) F. Meng, Y.-M. Hervault, Q. Shao, B. Hu, L. Norel, S. Rigaut, X. Chen, *Nat. Commun.* **2014**, *5*, 3023; b) L. Antonov, V. Deneva, S. Simeonov, V. Kurteva, D. Nedeltcheva, J. Wirz, *Angew. Chem.* **2009**, *121*, 8015 – 8018; *Angew. Chem. Int. Ed.* **2009**, *48*, 7875 – 7878; c) K. M. Kadish, W. E, R. Zhan, T. Khoury, L. J. Govenlock, J. K. Prashar, P. J. Sintic, K. Ohkubo, S. Fukuzumi, M. J. Crossley, *J. Am. Chem. Soc.* **2007**, *129*, 6576 – 6588.

[9] a) J. Braun, M. Koecher, M. Schlabach, B. Wehrle, H.-H. Limbach, E. Vogel, *J. Am. Chem. Soc.* **1994**, *116*, 6593 – 6604; b) H. Furuta, T. Ishizuka, A. Osuka, H. Dejima, H. Nakagawa, Y. Ishikawa, *J. Am. Chem. Soc.* **2001**, *123*, 6207 – 6208; c) Y. S. Xie, P. C. Wei, X. Li, T. Hong, K. Zhang, H. Furuta, *J. Am. Chem. Soc.* **2013**, *135*, 19119 – 19122.

[10] a) A. Shundo, J. P. Hill, K. Ariga, *Chem. Eur. J.* **2009**, *15*, 2486 – 2490; b) A. Shundo, J. Labuta, J. P. Hill, S. Ishihara, K. Ariga, *J. Am. Chem. Soc.* **2009**, *131*, 9494 – 9495; c) Y. S. Xie, J. P. Hill, A. L. Schumacher, P. A. Karr, F. D'Souza, C. E. Anson, A. K. Powell, K. Ariga, *Chem. Eur. J.* **2007**, *13*, 9824 – 9833.

[11] D. Lahaye, K. Muthukumaran, C.-H. Hung, D. Gryko, J. S. Rebouças, I. Spasojevic, I. Batinic-Haberle, J. S. Lindsey, *Bioorg. Med. Chem.* **2007**, *15*, 7066 – 7086.

[12] D. M. Shen, C. Liu, X. G. Chen, Q. Y. Chen, *Synlett* **2009**, 945 – 948.

[13] CCDC-981504 (**DPH_{22}**), -981505 (**DPH_{40}·2 DMF**), and -981506 (**$ZnDPH_{02}$·3 DMF**) contain the supplementary crystallographic data for this paper. These data can be obtained free of charge from The Cambridge Crystallographic Data Centre via www.ccdc.cam.ac.uk/data_request/cif.

[14] Q. G. Wang, Y. S. Xie, Y. B. Ding, X. Li, W. H. Zhu, *Chem. Commun.* **2010**, *46*, 3669 – 3671.

[15] a) Y. Liu, W. Jiang, H.-Y. Zhang, C.-J. Li, *J. Phys. Chem. B* **2006**, *110*, 14231 – 14235; b) X. Guo, D. Zhang, H. Tao, D. Zhu, *Org. Lett.* **2004**, *6*, 2491 – 2494; c) Z. Q. Guo, P. Zhao, W. H. Zhu, X. M. Huang, Y. S. Xie, H. Tian, *J. Phys. Chem. C* **2008**, *112*, 7047 – 7053; d) F. M. Raymo, R. J. Alvarado, S. Giordani, M. A. Cejas, *J. Am. Chem. Soc.* **2003**, *125*, 2361 – 2364; e) D. C. Magri, M. Camilleri Fava, C. J. Mallia, *Chem. Commun.* **2014**, *50*, 1009 – 1011.

[16] a) A. D. Becke, *J. Chem. Phys.* **1993**, *98*, 5648 – 5652; b) C. Lee, W. Yang, R. G. Parr, *Phys. Rev. B* **1988**, *37*, 785 – 789.

[17] W. J. Hehre, R. Ditchfield, J. A. Pople, *J. Chem. Phys.* **1972**, *56*, 2257 – 2261.

[18] J. Tomasi, B. Mennucci, R. Cammi, *Chem. Rev.* **2005**, *105*, 2999 – 3094.

[19] Gaussian 09, Revision A.02, M. J. Frisch, G. W. Trucks, H. B. Schlegel, G. E. Scuseria, M. A. Robb, J. R. Cheeseman, G. Scalmani, V. Barone, B. Mennucci, G. A. Petersson, H. Nakatsuji, M. Caricato, X. Li, H. P. Hratchian, A. F. Izmaylov, J. Bloino, G. Zheng, J. L. Sonnenberg, M. Hada, M. Ehara, K. Toyota, R. Fukuda, J. Hasegawa, M. Ishida, T. Nakajima, Y. Honda, O. Kitao, H. Nakai, T. Vreven, J. A. Montgomery, Jr., J. E. Peralta, F. Ogliaro, M. Bearpark, J. J. Heyd, E. Brothers, K. N. Kudin, V. N. Staroverov, R. Kobayashi, J. Normand, K. Raghavachari, A. Rendell, J. C. Burant, S. S. Iyengar, J. Tomasi, M. Cossi, N. Rega, J. M. Millam, M. Klene, J. E. Knox, J. B. Cross, V. Bakken, C. Adamo, J. Jaramillo, R. Gomperts, R. E. Stratmann, O. Yazyev, A. J. Austin, R. Cammi, C. Pomelli, J. W. Ochterski, R. L. Martin, K. Morokuma, V. G. Zakrzewski, G. A. Voth, P. Salvador, J. J. Dannenberg, S. Dapprich, A. D. Daniels, Ö. Farkas, J. B. Foresman, J. V. Ortiz, J. Cioslowski, D. J. Fox, Gaussian, Inc. Wallingford CT, **2009**.

Received: June 5, 2014
Published online on August 14, 2014